HHS Public Access

Author manuscript

Genesis. Author manuscript; available in PMC 2016 April 11.

Published in final edited form as:

Genesis. 2015 March ; 53(0): 285–293. doi:10.1002/dvg.22848.

A Cre-inducible fluorescent reporter for observing apical membrane dynamics

Xinchao Pan[1], **Ulrike Schnell**[1], **Courtney M. Karner**[2], **Erin V. Small**[1], and **Thomas J. Carroll**[1,*]

[1]Departments of Internal Medicine (Nephrology) and Molecular Biology, UT Southwestern Medical Center, Dallas, TX 75390-9148

[2]Department of Orthopedic Surgery, Washington University School of Medicine, St. Louis, MO, USA

Abstract

The ability to image living tissues with fluorescent proteins has revolutionized the fields of cell and developmental biology. Fusions between fluorescent proteins and various polypeptides are allowing scientists to image tissues with sub-cellular resolution. Here, we describe the generation and activity of a genetically engineered mouse line expressing a fusion between the green fluorescent protein (GFP) and the apically localized protein Crumbs3 (Crb3). This reporter drives Cre inducible expression of Crb3-GFP under control of the EF1a regulatory domains. The fusion protein is broadly expressed in embryonic and adult tissues and shows apical restriction in the majority of epithelial cell types. It displays a variably penetrant gain of function activity in the neural tube. However, in several cell types, over-expression of Crb3 does not appear to have any affect on normal development or maintenance. Detailed analysis of kidneys expressing this reporter indicates normal morphology and function highlighting the utility for live imaging. Thus, the EF1a$^{Crb3\text{-}GFP}$ mouse line will be of broad use for studying membrane and/or tissue dynamics in living tissues.

Keywords

morphogenesis; apical membrane; live imaging; membrane dynamics

Results and Discussion

The development of techniques that facilitate live imaging of cells and tissues has led to multiple paradigm shifting discoveries over the last decade. The generation of fluorescent proteins targeted to specific regions within the cell, including organelles, is allowing investigators to observe living tissue with sub-cellular resolution.

The plasma membrane of epithelial cells can roughly be divided into apical and basolateral domains separated by junctional complexes. The relative ratio of apical to basolateral membrane varies greatly depending on the cell type. For example, in the kidney, the

*Author for correspondence: Thomas.carroll@utsouthwestern.edu.

proximal tubules exhibit an extensive and complex apical membrane covered with microvilli, while the collecting ducts have a simple, relatively smooth apical membrane (Christensen, 1982; Marshansky *et al.*, 2002). In the last several years, it has become apparent that relative changes in the apical and basolateral membrane can have profound effects on cell behavior including impacting cell shape, proliferation rates and tissue morphogenesis (Sawyer *et al.*, 2010; Van IJzendoorn *et al*., 2004). The ability to study plasma membrane domain dynamics in real time will have a significant impact on several fields of biology. Although there are fluorescent mouse lines available that can be used to visualize the entire plasma membrane, such as myristoylated fluorescent proteins, to our knowledge, there are none that specifically label the apical membrane.

The crumbs family of transmembrane proteins localizes to and regulates the formation of the apical membrane domain (Gosens *et al.*, 2008). Previous studies have shown that injection of mRNA encoding a crumbs3-GFP (Crb3-GFP) fusion protein into Xenopus embryos results in apical localization of GFP (Chalmers *et al.*, 2005). We generated a similar construct consisting of a mouse Crb3 cDNA and eGFP. This construct was utilized to engineer a mouse line in which the Crb3-GFP fusion protein can be driven in any cell type in the presence of Cre recombinase. After cloning the Crb3-GFP cDNA downstream of a floxed triple-poly adenylation site, the entire cassette was cloned into a vector containing 5′ and 3′ homology arms for the mouse eukaryotic elongation factor 1 alpha (from hereon referred to as EF1a) and a promoterless neomycin resistance gene (Figure 1A). Due to the lack of a promoter in the neomycin cassette, embryonic stem (ES) cells are only neomycin resistant if the targeting construct undergoes homologous recombination at the EF1a locus or a random integration event that results in pirating of a promoter element that drives expression in the ES cells. Random integration events will not result in drug resistance thus increasing the odds of selecting homologous recombinants. Indeed, out of 40 ES cell lines that were screened by Southern blot with probes to the 5′ and 3′ region, 39 appeared to have undergone homologous recombination.

Three of the targeted ES cell lines were injected into blastocysts and chimeric males were generated and bred to C57Bl6 females. Germline transmission of all three lines was confirmed via Southern blot of DNA from F1 offspring (not shown). After confirmation of homologous recombination, PCR of genomic DNA using sequence specific primers was used for all subsequent genotyping (Figure 1B). We will refer to this recombined allele as $EF1a^{Crb3\text{-}GFP/+}$. F1 $EF1a^{Crb3\text{-}GFP/+}$ females ($EF1a^{Crb3\text{-}GFP/Crb3\text{-}GFP}$ animals were not viable) were bred to males transgenic for Sox2Cre. Sox2Cre is active throughout the mouse epiblast at E6.5 (Hayashi *et al.*, 2002). Litters were collected at E11.5, 12.5, 13.5, 14.5, 15.5, P1 and P14. Sox2Cre;$EF1a^{Crb3\text{-}GFP/+}$ embryos and pups were easily identified using a fluorescent stereoscope as they expressed visually detectable levels of GFP (Figure 2 and data not shown). In the absence of Cre recombinase, GFP was undetectable in the $EF1a^{Crb3\text{-}GFP/+}$ embryos (Figure 2 and data not shown).

At E11.5, Sox2Cre;$EF1a^{Crb3\text{-}GFP/+}$ embryos were present at close to expected numbers (21% actual vs. 25% expected, Figure 2I). However, several E11.5 and E12.5 Sox2Cre;$EF1a^{Crb3\text{-}GFP/+}$ embryos showed neural tube defects including holoprosencephaly and spina bifida (Figure 2B, D, F and data not shown). By E12.5, we recovered significantly

fewer double heterozygous animals (14%) than expected (25%) and a high percentage showed neural tube defects (Figure 2I). The number of observed Sox2Cre;EF1a$^{Crb3\text{-}GFP/+}$ embryos declined slightly between E12.5 and 15.5 but a significant drop in viability took place between E15.5 and birth (Figure 2I). Out of 173 P1 pups collected, only 8 were Sox2Cre;EF1a$^{Crb3\text{-}GFP/+}$ positive (4.6% vs. 25% expected) even though the majority showed no overt signs of neural tube defects. No Sox2Cre;EF1a$^{Crb3\text{-}GFP/+}$ pups survived past P14. Importantly, at every stage examined, the surviving Sox2Cre;EF1a$^{Crb3\text{-}GFP/+}$ embryos or pups expressed GFP in multiple tissues indicating that surviving pups did not lack Crb3-GFP expression.

E11.5 and 12.5 Sox2Cre;EF1a$^{Crb3\text{-}GFP/+}$ embryos were collected, fixed, sectioned and stained with Hematoxylin and Eosin (H&E). Other than the low penetrance neural tube defects, there were no gross malformations in any of the major organ systems (Figure 2G, 2H and data not shown). Thus, the cause of lethality is still not clear.

To characterize EF1a$^{Crb3\text{-}GFP/+}$ expression, E12.5 embryos were sectioned and stained with antibodies to GFP and cellular markers including the basolateral protein E-cadherin (Figure 3) and the apical membrane marker aPKC (not shown). GFP was enriched at or restricted to the apical membrane of the majority of embryonic epithelial organs including the neural tube, vomeronasal epithelium, lens of the eye, nasal cavity, cochlea, telencephalon, pituitary, intestines, stomach, esophagus, trachea, lungs, pancreas (Figure 3 and not shown) and kidney (Figure 4 and 5). GFP expression was apparent in the retina of the eye and the liver; however, it did not appear to be apically localized (Figure 3B and H). We did not detect expression of GFP in most of the epidermis or in endothelial cells. Whether this is from a lack of EF1a expression or Crb3-GFP stability in these tissues is unknown.

As mentioned, Sox2Cre mediated activation of Crb3-GFP results in pre- and perinatal mortality suggesting that the EF1a$^{Crb3\text{-}GFP}$ allele has some gain of function activity. To test if there is gain of function activity in all cell types, we generated embryos expressing Crb3-GFP within the developing kidney. Previous studies found that overexpression of Crb3 in kidney cell lines leads to expanded apical membrane formation and Crb3 has been implicated in the regulation of luminal diameter and cyst formation in kidney tubules (Lemmers et al., 2004; Schlüter *et al.*, 2009). To determine if Crb3-GFP affects kidney epithelial development, we utilized the Sox2Cre line as well as two additional Cre lines that are expressed in a more restricted manner: Six2Cre and Hoxb7Cre. As mentioned, due to its activation in the epiblast, Sox2Cre should drive Crb3-GFP expression in the derivatives of all cell types in which Ef1a was expressed (Figure 4B, J, N). Six2Cre should drive expression within the nephron progenitor cells and their derivatives (Kobayashi *et al.*, 2008, Figure 4C, K, O) while Hoxb7Cre should activate expression in the Wolffian duct and its derivatives, the ureteric bud and collecting ducts (Yu *et al.*, 2002, Figure 4D, L, P).

In contrast to the Sox2Cre;EF1a$^{Crb3\text{-}GFP/+}$ results, Six2Cre;EF1a$^{Crb3\text{-}GFP/+}$ and Hoxb7Cre;EF1a$^{Crb3\text{-}GFP/+}$ mice were born at the expected Mendelian ratio and survived to adulthood. Mature adults showed no signs of increased mortality or decreased fertility (Figure 2I and not shown). Other than a slight reduction in kidney size observed in the

Sox2Cre;EF1a$^{Crb3\text{-}GFP/+}$ P1 pups that corresponded to a reduction in body size, the kidneys of all three genotypes appeared normal as assessed by H&E staining (Figure 4E–H).

To determine if the EF1a$^{Crb3\text{-}GFP/+}$ kidneys differentiated properly, we performed immunostaining on sectioned organs using an antibody to GFP. To determine differentiation status, we co-stained P1 kidneys with markers of the collecting ducts and proximal tubules (Dolichos biflorus agglutinin, DBA, or Lotus tetragonolobus lectin, LTL, respectively) as these cell types are derivatives of Hoxb7Cre or Six2Cre expressing cells. In Sox2Cre;EF1a$^{Crb3\text{-}GFP/+}$ kidneys, GFP expression was most prominent in epithelial structures including the collecting ducts and proximal tubules although expression was also evident in non-epithelial tissues such as the cap mesenchyme and stroma (Figures 4J, N and 5B, F and F′). No GFP was observed in the renal vasculature (not shown). There was no discernible difference in the density, length or diameter of proximal tubules or collecting ducts relative to the wild type control (compare Figure 4A, I, M to Figures 4J, N). In the Six2Cre;EF1a$^{Crb3\text{-}GFP/+}$ kidneys, GFP was evident in the cap mesenchyme (nephron progenitor cells) and their derivatives throughout the embryonic period (Figures 4K, O and 5C, G and G′ and not shown). No defect in the formation or differentiation of the nephrons was observed. In some kidneys, we did observe apical GFP within the E-cadherin positive tips of the ureteric bud (see white arrow in Figure 5G, G′ and G″). This most likely is the result of the fact that there is some mixing of cells derived from the cap mesenchyme and the UB when the developing nephron fuses to the UB (Qiao *et al.*, 1995). In the Hoxb7Cre;EF1a$^{Crb3\text{-}GFP/+}$ kidneys, GFP was specifically expressed in the ureteric bud and collecting ducts (Figures 4L, P and 5D, H and H′). No defects in UB branching morphogenesis or diameter were detected. Taken together with the fact that the Six2Cre;EF1a$^{Crb3\text{-}GFP/+}$ and Hoxb7Cre;EF1a$^{Crb3\text{-}GFP/+}$ mice have a normal lifespan, these data suggest that over- and misexpression of Crb3-GFP does not result in defects within the developing and or adult kidney.

We next performed a more detailed analysis of the expression of the Crb3-GFP fusion protein in the kidney. In the Sox2Cre line, GFP protein was present in small domains within the non-epithelial metanephric mesenchyme (Arrows in Figures 5B, F, and F′). This focal expression was observed in both the cap mesenchyme (as visualized by co-labeling with an antibody to Six2) and the cortical stroma (Figure 5B). Similar punctate expression was observed in the Six2Cre;EF1a$^{Crb3\text{-}GFP/+}$ mesenchyme although it was limited to the cap mesenchyme (Arrows in Fig. 5C, G and G′). No mesenchymal expression of GFP was observed in the Hoxb7Cre;EF1a$^{Crb3\text{-}GFP/+}$ cap mesenchyme (Figure 5D, H and H′).

As the nephron progenitors underwent mesenchymal to epithelial transition, the punctate expression of GFP within the nephron progenitors decreased while expression at cell-cell junctions became apparent in the Six2Cre;EF1a$^{Crb3\text{-}GFP/+}$ and Sox2Cre;EF1a$^{Crb3\text{-}GFP/+}$ kidneys (Arrowheads in Figure 5F, G, F′, G′ F″ and G″). In more mature nephron structures, GFP was localized to the lumenal side of the epithelia (Figure 4N and O). Co-staining with an antibody to the apical membrane marker aPKC showed a high degree of overlap in localization of these two proteins (Figure 5F, G, F′, G′ F″ and G″). No differences in luminal diameter were noted nor was the apical membrane domain expanded in Six2Cre or Sox2Cre derived epithelia (Figures 4 and 5 and not shown).

We also examined the sub-cellular localization of Crb3-GFP protein in the Hoxb7Cre;EF1a$^{Crb3\text{-}GFP/+}$ line (Figure 5D, H, H′ and H″). GFP always co-localized with aPKC and there was little to no overlap with the adherens junction protein E-cadherin, even at the newly forming UB tips. Unlike the observations in the developing nephrons, we never observed Crb3-GFP protein in punctate structures or at cell-cell junctions in the ureteric bud or collecting ducts. The identity of the punctate, GFP positive structures is not known although they may represent membrane bound vesicles or the recently described pre-apical domains that are observed in the nephrons prior to epithelialization (Yang *et al.*, 2013). Why they are not present in branching UB is not known although it most likely is a reflection of the differences in the way the two epithelial types develop (mesenchymal to epithelial transition vs. branching morphogenesis). As was observed for the Sox2Cre and Six2Cre lines, there was no difference in epithelial cell diameter in the Hoxb7Cre;EF1a$^{Crb3\text{-}GFP/+}$ kidneys. The lack of a morphological defect along with the normal viability in kidney epithelia mis-/overexpressing Crb3 suggest this allele has no gain of function activity in this organ. Potential explanations for the discrepancy in our observations compared to previous findings in cells expressing Crb3 may indicate that the fusion protein produced from the EF1a locus is non-functional or that it is expressed at levels too low to elicit a gain of function effect.

As the EF1a$^{Crb3\text{-}GFP/+}$ line has no gain of function activity within the kidney, we next tested whether it would be of use for live imaging of apical membrane dynamics. Six2Cre;EF1a$^{Crb3\text{-}GFP/+}$ and Hoxb7Cre;EF1a$^{Crb3\text{-}GFP/+}$ urogenital systems were dissected from E12.5 embryos and cultured at the air-media interface for up to 72 hours. Images were captured every 24 hours for 3 days. Crb3-GFP was expressed in both lines at high enough levels to be captured using a fluorescent stereomicroscope with no effects on development relative to unimaged contralateral kidneys (Figure 6A–F and data not shown) indicating that this line can be used for low resolution studies of tissue morphogenesis.

We next performed a high-resolution analysis of Hoxb7Cre;EF1a$^{Crb3\text{-}GFP/+}$; Rosa26-Tomato kidneys. Cultured organs were imaged with a 20× objective on a confocal microscope equipped with a stagetop tissue incubator. Z-stacks were captured at 2 μm intervals for both GFP and Tomato every 20 minutes for 20 hours. The total scan time for each timepoint was approximately 2 minutes. In a subset of ureteric buds, signs of cell death were apparent after 12 hours (arrowheads in Figure 6J-L). This death appeared to be the result of phototoxicity as unscanned tissues in the same incubator showed no signs of death (not shown). However, for most UBs, development proceeded normally for the entire imaging period and we were able to collect high-resolution images of the kidney lumen as it formed. In Figure 6G–L, we show maximum projection reconstructions of z-stacks at 4 hour intervals. Interestingly, protrusion of the apical membrane towards the basal side of the cell was apparent at the future sites of branching morphogenesis prior to any signs of branching or noticeable deformation of the basolateral aspect of the epithelium (arrows in Figure 6G–L). This observation suggests the intriguing possibility that luminal expansion drives UB branching morphogenesis. This possibility needs to be further investigated. However, the data presented clearly demonstrate that the EF1a$^{Crb3\text{-}GFP/+}$ line is suitable for live imaging apical membrane dynamics in complex, 3-D tissues.

Methods

Plasmid Construct

To generate a Crb3-GFP c-terminal fusion protein, a full-length cDNA for mouse Crumbs 3 was amplified by PCR and cloned into pEGFP-N3 vector (Clontech, CA). This Crb3-GFP cDNA was sub-cloned into the pSA-lox-Neo-TPA shuttle vector that possesses a promoterless Neomycin resistance cassette. The lox-Neo-TPA-Crb3-GFP insert was released by digestion with Pac1 and Asc1 and cloned into a vector containing homology arms to EF1alpha flanking PacI and AscI cloning sites (kindly provided by Argiris Efstratiadis, Columbia University).

EF1a$^{Crb3\text{-}GFP/+}$ floxed mice

The EF1alpha-lsl-Crb3-GFP construct was linearized with Ahd1, purified using Elutip D columns (Whatman, Florham Park, NJ) and electroporated into mouse embryonic stem cells. After electroporation, the cells were cultured in the presence of neomycin. Genomic DNA was isolated from 40 Neo resistant ES cell colonies, digested with BamHI. A Southern blot of digested DNA was screened using probes 5′ and 3′ to the EF1a locus. 39/40 clones screened appeared to have undergone homologous recombination at the EF1alpha locus. Three clones were amplified and injected into blastocysts. All three showed germline transmission.

F1 offspring from each of the three chimeric lines was crossed to Hoxb7Cre mice to assess activity of the Crb3-GFP transgene. All three showed expression on the apical side of the mouse collecting ducts from the earliest stages examined (E11.5) into adult stages as would be expected with Hoxb7Cre activity (Yu *et al.*, 2002). One line was used for all further analysis. EF1a$^{Crb3\text{-}GFP/+}$ mice were genotyped using specific primers 5′-TTTGGTTTGCCGATGCTGC-3′ and 5′-GGACTCCCAGAATGGAAAAGACC-3′ resulting in a 154bp DNA product. EF1a$^{Crb3\text{-}GFP/+}$ females were crossed with Six2Cre or Sox2Cre males to test the expression (Kobayashi *et al.*, 2008; Hayashi *et al.*, 2002). Females were separated on the day of vaginal plug and dissected at the time indicated. For calculation of survival curves, embryos and pups were collected at the stages indicated. The percentage of surviving animals with two transgenic alleles was calculated as the ratio of observed numbers to expected numbers. At least three litters from each genotype were collected at each timepoint. The ratios of observed to expected numbers of embryos/pups are as follows, Hoxb7Cre;EF1a$^{Crb3\text{-}GFP/+}$: 15/16 at E11.5, 18/16 at E12.5, 7/7.5 at E14.5, 12/12.25 at E15.5, 20/18.25 at P1 and 56/55.5 at P14. Six2Cre;EF1a$^{Crb3\text{-}GFP/+}$: 6/5.75 at E11.5, 8/7.75 at E12.5, 8/8.07 at E14.5, 16/16.5 at E15.5, 11/10.5 at P1 and 47.5/54.5 at P14. Sox2Cre;EF1a$^{Crb3\text{-}GFP}$: 14/17 at E11.5, 19/35 at E12.5, 3/6.5 at E14.5, 7/19.5 at E15.5, 8/43.25 at P1, 0/17.25 at P14.

Ex Vivo Organ Culture

Organ culture was described previously (Pan *et al.*, 2013). Briefly, kidneys were dissected out at E12.5 and grown on transwell filters (Whatman, Florham Park, NJ) at the air/media interface. Pictures were taken on a Zeiss NeoLumar stereoscope using an Olympus DP71

camera every 24 h. All experiments were repeated at least three times with a minimum of six individual kidneys from six distinct embryos assayed per replicate.

Live cell imaging

Rosa26-Tomato females were crossed with Hoxb7Cre;EF1a$^{Crb3\text{-}GFP/+}$ males and kidneys were dissected out at E13.5 (Madisen *et al.*, 2010). Kidneys were plated on a thin Matrigel layer (1:4 in medium; BD Biosciences, Franklin Lakes, NJ) in Lab-Tek Chambered #1.0 Borosilicate Coverglass System dishes (Nalge Nunc International, Rochester, NY). Additional medium was added to surround half of the kidney, allowing growth at the air/media interface. Four kidneys were cultured and two of them were imaged at 20× magnification. Pictures were taken every 20 min for 20 h using a Nikon A1 laser scanning confocal microscope with a Tokai Hit stage Top incubator (Tokai Hit Co., Shizuoka, Japan).

Immunostaining

Embryos or kidneys were fixed overnight in 4% paraformaldehyde (PFA) at 4°C with gentle agitation. After being cryoprotected in 30% sucrose, the specimens were embedded in OCT and cryosectioned at 10 μm thickness. Sections were washed three times in 0.1% Triton-X/PBS for 5 min each wash and blocked for a minimum of 1 hr at room temperature in 5% FBS/0.1% Triton-X/PBS. Sections were incubated in primary antibody at 4 degrees overnight followed by 3 washes in 0.1% Triton-X/PBS. Sections were then incubated in secondary antibody for 2 hr at room temperature, washed 3 times in PBS, mounted with Vectashield, and examined by scanning laser confocal microscopy (Zeiss LSM-510). The primary antibodies used are anti-GFP (chicken; 1:1000, AvesLabs), anti-E-cadherin (Mouse, 1:500, BD Biosciences, CA), anti-Six2 (Rabbit, 1:250, ProteinTech), anti-aPKC (rabbit; 1:500, Santa Cruz, CA), anti-DBA (Biotinylated; 1:500, VectorLabs, Burlingame, CA), anti-LTL (Biotinylated, 1:500, VectorLabs, Burlingame, CA). Nuclei were stained with Topro-3 iodide (1:1,000, Invitrogen). Results shown are representative examples from one of at least three different stainings of three different embryos. We used either Cre positive;EF1a$^{+/+}$ or Cre negative; EF1a$^{Crb3\text{-}GFP/+}$ tissues as controls.

H&E histology

Kidneys from P1 pups were fixed with 4% PFA and embedded in paraffin. The kidneys were then sectioned and stained with H&E using standard techniques.

Acknowledgments

The authors would like to thank Callie Kwartler for reading and commenting on this manuscript. This work was supported by the UT Southwestern O'Brien Kidney Research Center (P30DK079328). XP was supported by a post-doctoral fellowship from the National Kidney Foundation. Work in the Carroll lab is supported in part by the NIH (RO1DK080004, RO1DK095057) and Cell Lineage and Differentiation Research Grant No. 1-FY11-514 from the March of Dimes Foundation.

References

Chalmers AD, Pambos M, Mason J, Lang S, Wylie C, Papalopulu N. aPKC, Crumbs3 and Lgl2 control apicobasal polarity in early vertebrate development. Development. 2005; 132(5):977–86. [PubMed: 15689379]

Christensen EI. Rapid membrane recycling in renal proximal tubule cells. Eur J Cell Biol. 1982; 29(1): 43–9. [PubMed: 7151825]

Hayashi S, Lewis P, Pevny L, McMahon AP. Efficient gene modulation in mouse epiblast using a Sox2Cre transgenic mouse strain. Mech Dev. 2002; 119(Suppl 1):S97–S101. [PubMed: 14516668]

Gosens I, den Hollander AI, Cremers FP, Roepman R. Composition and function of the Crumbs protein complex in the mammalian retina. Exp Eye Res. 2008; 86(5):713–26. [PubMed: 18407265]

Kobayashi A, Valerius MT, Mugford JW, Carroll TJ, Self M, Oliver G, McMahon AP. Six2 defines and regulates a multipotent self-renewing nephron progenitor population throughout mammalian kidney development. Cell Stem Cell. 2008; 7;3(2):169–81.

Lemmers C, Michel D, Lane-Guermonprez L, Delgrossi MH, Médina E, Arsanto JP, Le Bivic A. CRB3 binds directly to Par6 and regulates the morphogenesis of the tight junctions in mammalian epithelial cells. Mol Biol Cell. 2004; 15(3):1324–33. [PubMed: 14718572]

Madisen L, Zwingman TA, Sunkin SM, Oh SW, Zariwala HA, Gu H, Ng LL, Palmiter RD, Hawrylycz MJ, Jones AR, Lein ES, Zeng H. A robust and high-throughput Cre reporting and characterization system for the whole mouse brain. Nat Neurosci. 2010; 13(1):133–40. [PubMed: 20023653]

Marshansky V, Ausiello DA, Brown D. Physiological importance of endosomal acidification: potential role in proximal tubulopathies. Curr Opin Nephrol Hypertens. 2002; 11:527–537. [PubMed: 12187318]

Pan X, Small EV, Igarashi P, Carroll TJ. Generation and characterization of KsprtTA and KsptTA transgenic mice. Genesis. 2013; 51(6):430–5. [PubMed: 23420736]

Qiao J, Cohen D, Herzlinger D. The metanephric blastema differentiates into collecting system and nephron epithelia in vitro. Development. 1995 Oct; 121(10):3207–14. [PubMed: 7588055]

Sawyer JM, Harrell JR, Shemer G, Sullivan-Brown J, Roh-Johnson M, Goldstein B. Apical constriction: a cell shape change that can drive morphogenesis. Dev Biol. 2010; 1;341(1):5–19.

Schlüter MA, Pfarr CS, Pieczynski J, Whiteman EL, Hurd TW, Fan S, Liu CJ, Margolis B. Trafficking of Crumbs3 during cytokinesis is crucial for lumen formation. Mol Biol Cell. 2009; 20(22):4652–63. [PubMed: 19776356]

Van IJzendoorn SC, Théard D, Van Der Wouden JM, Visser W, Wojtal KA, Hoekstra D. Oncostatin M-stimulated apical plasma membrane biogenesis requires p27(Kip1)-regulated cell cycle dynamics. Mol Biol Cell. 2004; 15(9):4105–14. [PubMed: 15240818]

Yang Z, Zimmerman S, Brakeman PR, Beaudoin GM 3rd, Reichardt LF, Marciano DK. De novo lumen formation and elongation in the developing nephron: a central role for afadin in apical polarity. Development. 2013; 140(8):1774–84. [PubMed: 23487309]

Yu J, Carroll TJ, McMahon AP. Sonic hedgehog regulates proliferation and differentiation of mesenchymal cells in the mouse metanephric kidney. Development. 2002; 129(22):5301–12. [PubMed: 12399320]

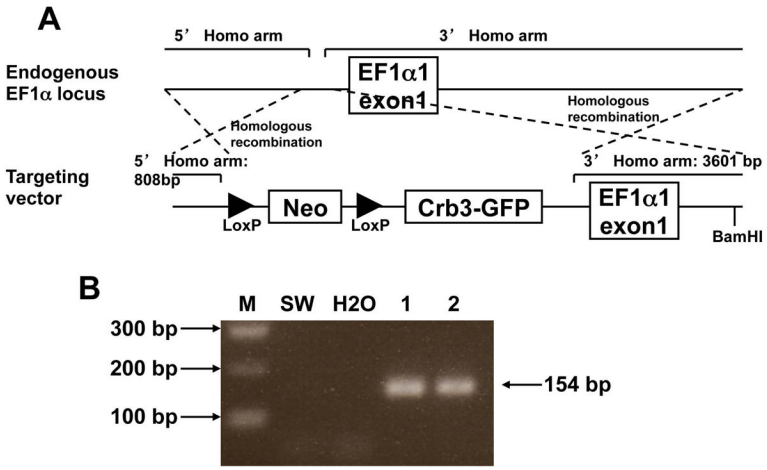

Figure 1. Generation of a Cre-inducible Crb3-GFP knock-in mouse line

A, Diagram depicting the targeting strategy used to introduce the Crb3-GFP cassette into exon1 of the EF1a locus by homologous recombination in ES cells; B, PCR genotyping indicates the presence of the Crb3-GFP cassette only in DNA obtained from transgenic mice 1 and 2 but not in DNA from a control Swiss Webster mouse (SW). (M, DNA marker)

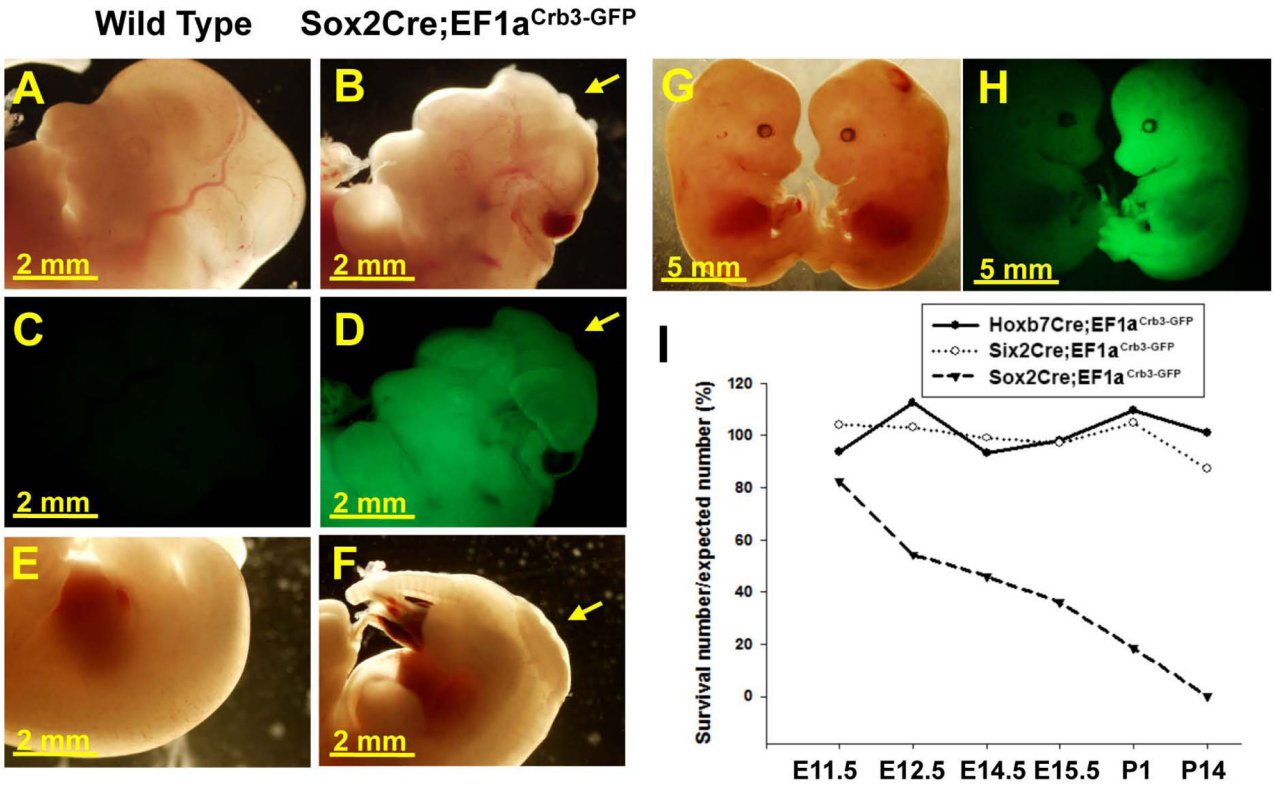

Figure 2. Sox2Cre-induced overexpression of Crb3-GFP leads to neural tube defects

A–F, E12.5 Sox2Cre;EF1a $^{Crb3\text{-}GFP/+}$; wild type (A, C, E) and mutant (B, D, F) embryos were photographed under incandescent and fluorescent light. The arrows indicate the open neural tube in the head (B, D) and around the tail (F) in mutant embryos. G and H, E14.5 wild type (left) and mutant (right) embryos were photographed under incandescent (G) and fluorescent (H) light. I, Survival curve of mice with Crb3-GFP overexpression induced by different Cre lines.

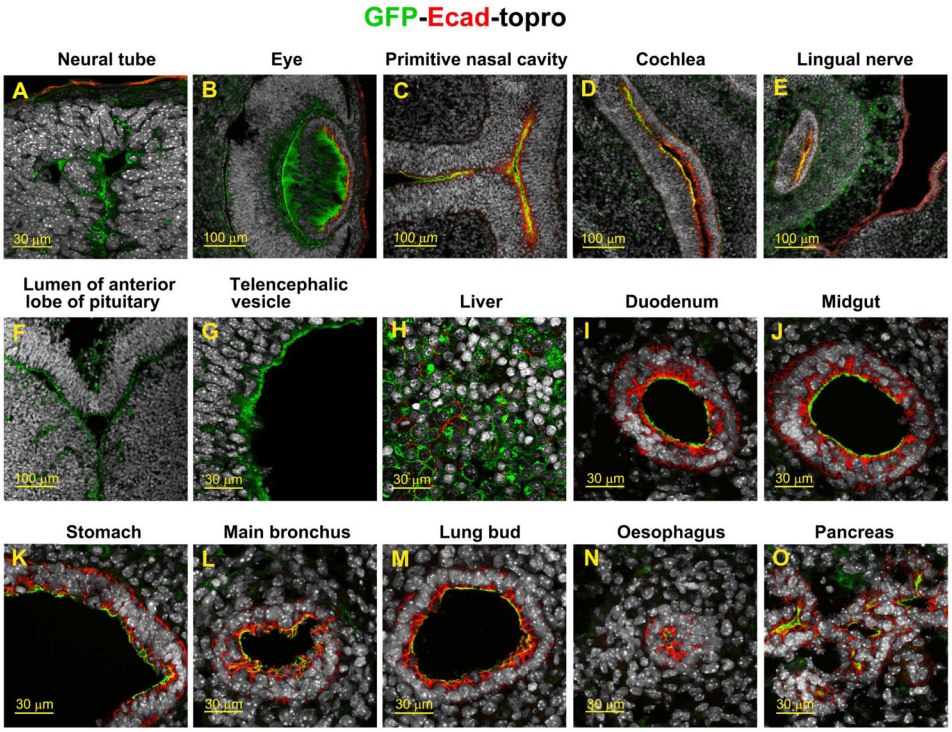

Figure 3. Crb3-GFP expression in different tissues of Sox2Cre;EF1a$^{Crb3\text{-}GFP/+}$ embryos

Sections of E12.5 Sox2Cre;EF1a$^{Crb3\text{-}GFP/+}$ embryos. Every tenth section of the whole embryo was stained with antibodies to GFP (green), E-cadherin (red) and Topro-3 (gray, nucleus).

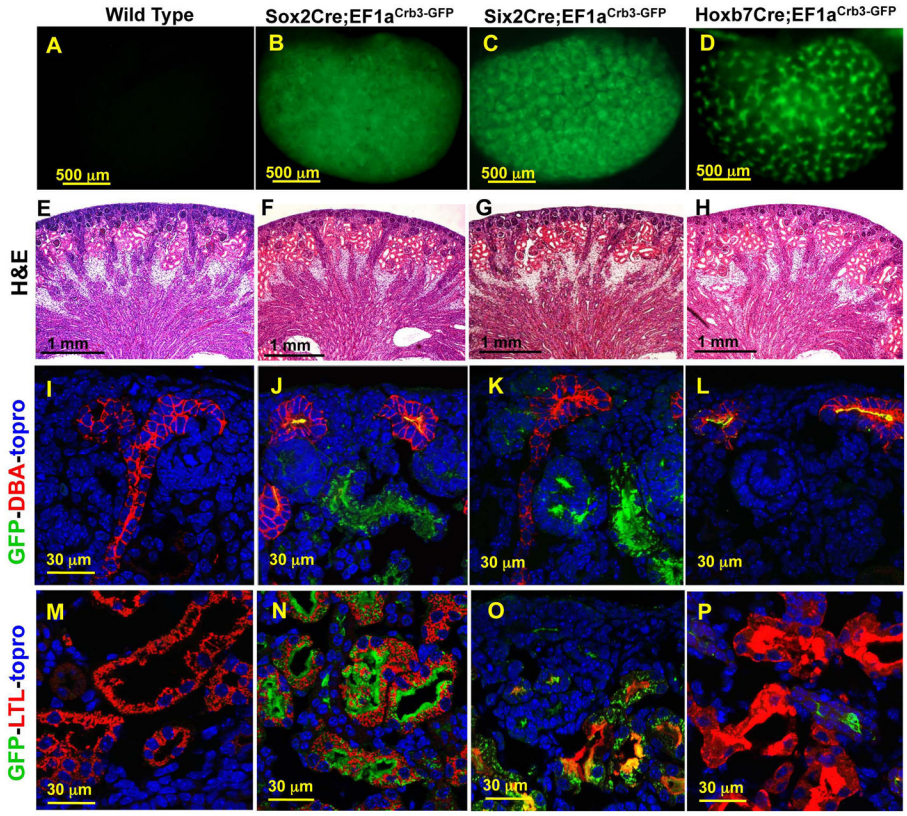

Figure 4. Histology and localization of GFP in distinct kidney segments

A–D, Wholemount images of wild-type (A) Sox2Cre-(B), Six2Cre-(C) and Hoxb7Cre-(D); EF1a$^{Crb3\text{-}GFP/+}$ E15.5 kidneys visualized by fluorescent microscopy. Images were taken using the same exposure time and magnification. E–H, H&E stained sections of P1 kidneys. I-P, sections of P1 kidneys stained with antibodies to GFP (green), the collecting duct marker DBA (red in I–L) or proximal tubule marker LTL (red in M–P) and the nuclear marker Topro-3 (blue).

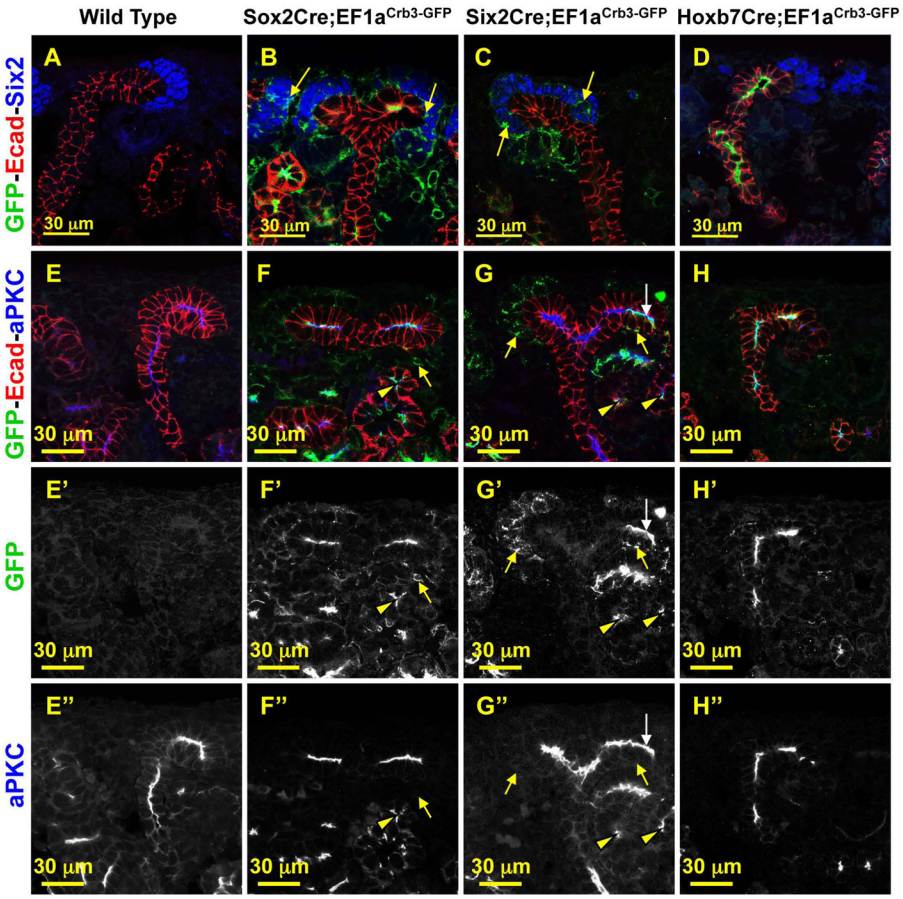

Figure 5. Apical GFP localization in Crb3-GFP expressing kidneys

A–D, P1 kidney sections stained with antibodies to GFP (green), E-cadherin (red) and Six2 (blue). E–H, P1 kidney sections stained with antibodies to GFP (green), E-cadherin (red) and aPKC (blue). Single channels of GFP and aPKC are shown in E′–H′ and E″–H″, respectively. Yellow arrows indicate the punctate expression of GFP within the non-epithelial metanephric mesenchyme. White arrows show GFP expression in ureteric bud tips. Arrowheads indicate co-expression of GFP and aPKC at cell-cell junctions.

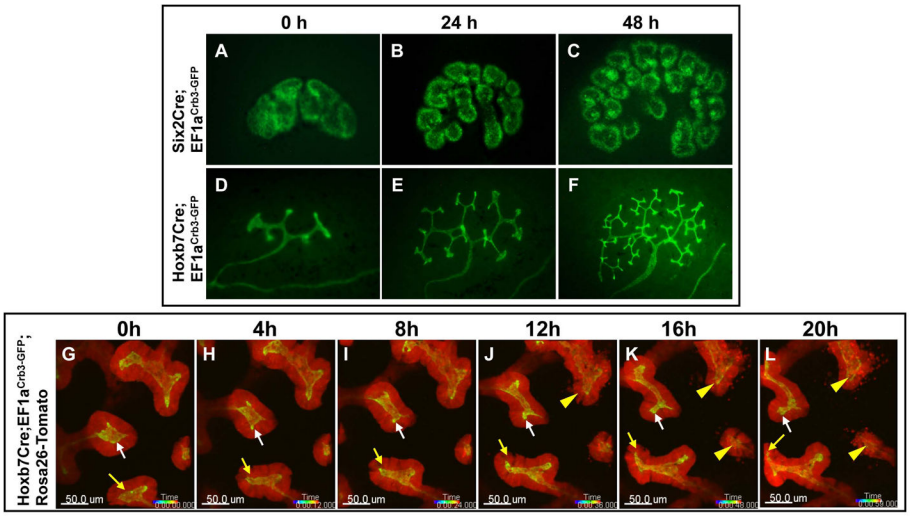

Figure 6. Live imaging of ex vivo cultured Crb3-GFP expressing embryonic kidneys

A–F, Six2Cre;EF1a$^{Crb3\text{-}GFP/+}$ (A–C) and Hoxb7Cre;EF1a$^{Crb3\text{-}GFP/+}$ (D–F) kidneys were collected at E12.5 and cultured for 48h. Pictures were taken every 24h. G–L, Hoxb7Cre; EF1a$^{Crb3\text{-}GFP/+}$;Rosa26-Tomato kidneys were collected at E13.5 and imaged live with an inverted confocal microscope. Z-stacks were taken every 20 min for a total of 20 hrs. Images represent a maximum projection reconstruction of 30 2 μm sections captured for both the GFP and Tomato channels. Arrows indicate the basally protruding apical membrane. The arrowheads indicate tubular death.